Dynamically screened electron–electron scattering in two dimensions

2003 J. Phys.: Condens. Matter 15 1057

(http://iopscience.iop.org/0953-8984/15/7/304)

INSTITUTE OF PHYSICS PUBLISHING JOURNAL OF PHYSICS: CONDENSED MATTER

J. Phys.: Condens. Matter **15** (2003) 1057–1069 PII: S0953-8984(03)55112-8

Dynamically screened electron–electron scattering in two dimensions

P Tripathi and B K Ridley

Department of Electronic Systems Engineering, University of Essex, Colchester, UK

Received 22 October 2002
Published 10 February 2003
Online at stacks.iop.org/JPhysCM/15/1057

Abstract

The properties of dynamically screened electron–electron interactions in a two-dimensional and quasi-two-dimensional semiconductor are described analytically for the situation where the electron gas obeys classical statistics. The electron–electron interaction is taken to be screened by the polar lattice and by free electrons in the lowest subband. The character of the screening is shown to be critically dependent on the energy and momentum exchanged in the electron–electron interaction. A remarkable feature is the resonant enhancement of the interaction strength by coupled-phonon–plasmon mode effects. As a consequence, the coupled-mode enhancement of the electron–electron energy exchange rate offers substantial competition to the energy-relaxation rate of electrons via optical-phonon emission.

1. Introduction

Electron–electron scattering in quasi-two-dimensional semiconductors has been the topic of considerable research over the last 20 years or so [1–12]. One motivation for this has been to understand its role in phenomena such as the quantum Hall effect and localization effects at extremely low temperatures [13]. Another motivation has been to quantify its effect on transport properties, and it is in this context that the present paper is written.

Although electron–electron (ee) scattering by itself cannot relax the drift momentum and energy gained from an electric field, it can, by randomizing these dynamic quantities within the electron gas, affect the distribution function in the presence of a field and thereby affect the transport properties, particularly at high fields. A well-known example of this is the establishment of an electron temperature distinct from the lattice temperature that quantifies a Fermi–Dirac or Maxwell–Boltzmann distribution. The condition for this to occur is simply that the rate of energy exchange in ee collisions greatly exceeds the rate of energy relaxation processes via other scattering mechanisms. In principle, it is also possible for momentum exchange in ee scattering to dominate and this condition would lead to a drifted distribution, i.e. one centred downstream of $\boldsymbol{k} = 0$, where $\boldsymbol{k}$ is the wavevector. Indeed, in the early days of the study of hot-electron transport in bulk polar semiconductors, the production of a

0953-8984/03/071057+13$30.00

drifted Maxwellian distribution was a common assumption [14, 15]. However, this assumption was soon abandoned, at least for bulk material, once it became clear that a sufficiently high electron concentration entailed a corresponding high concentration of charged impurities and, in consequence, a high momentum-relaxation rate. But because charged-impurity scattering is elastic it was still possible to assume that an electron temperature could be established, and in many cases this was observed [16].

The situation in quasi-two-dimensional structures is radically different: the concentration of electrons in a quantum well can be manipulated separately from the impurity concentration. In zinc-blende-type heterostructures, e.g. AlGaAs/GaAs, the electron gas can be derived from remote impurities via the technique of modulation doping. In wurtzite-type heterostructures, e.g. AlGaN/GaN, the electrons derive from spontaneous polarization and from any residual impurities [17–19]. In the former case the extra momentum relaxation introduced by the presence of charged impurities is much reduced, as evidenced by the observation of impressively large mobilities at low temperatures. In the nitride case scattering by charged impurities can, in principle, be eliminated completely. Thus, in quasi-2D structures there exists the possibility that a drifted distribution is possible under practical conditions. A recent study of this case has led to predictions of novel hot-electron phenomena, including squeezed electrons and absolute cooling [20]. Most studies of hot-electron transport have been carried out for the room temperature case in the context of Monte Carlo simulations [21] in which ee scattering is notoriously difficult to model. Moreover, at room temperature, energy and momentum relaxation via scattering by optical phonons is often dominant. There is, therefore, considerable scope for further study of hot-electron transport in quasi-2D structures, especially at lattice temperatures low enough for optical-phonon scattering to be negligible. We have reported such a study for the case of transport at 77 K in AlGaN/GaN and have concluded that a hot-electron drifted Maxwellian distribution is possible [22].

In what follows we examine the dynamics of ee scattering. The study of ee scattering in quasi-2D structures has been the topic of a number of papers, as we have already noted, but, in most, the ee interaction has been assumed to be screened statically, which is only correct for quasi-elastic collisions. In some studies employing Monte Carlo techniques, details of the interaction are entirely hidden, whether static or dynamic screening is assumed. It is, however, now generally accepted that the ee interaction is, in general, dynamically screened [23–27]. Here, we give an analytic/numerical description of energy and momentum exchange via the dynamically screened ee interaction in a polar lattice. We show that energy-exchange rates show distinct resonances at the coupled-mode frequencies and trace this to the critical dependence of dynamic screening on the energy exchange. As concrete examples we provide quantitative measures for electrons in GaN and GaAs for comparison with phonon rates.

2. Theory

Our approach follows that of [26] which we outline here for convenience. We will regard the rate of electron–electron scattering by electrons with the same spin as negligible because of exchange and interference effects. The energy exchange rate can then be obtained by ignoring spin and treating the interaction as a simple two-body collision in which an incident electron, wavevector $\boldsymbol{k}_1$, collides with a target electron, wavevector $\boldsymbol{k}_2$, and after collision the electrons have wavevectors $\boldsymbol{k}_1'$ and $\boldsymbol{k}_2'$. The frequency of this process is calculated as usual in the Born approximation assuming that the electrons are confined before and after scattering in the lowest subband, taken to be parabolic. The physically meaningful rates are momentum and energy exchange rates rather than simple scattering rates, which means that the order of summation must be such that the final sum should be over one of the final states suitably weighted by

the amount of energy or momentum exchanged, i.e. by multiplying the integrand by $E_1 - E_1'$ for energy loss and by $\hbar(\boldsymbol{k}_1 - \boldsymbol{k}_1')$ for momentum loss. The calculation we give is of the rate of energy exchange. When the energy exchanged is significantly large the rate will be also approximately equal to the momentum exchange rate.

In order to be directly relevant to most hot-electron cases the calculation assumes non-degenerate statistics and essentially follows the analytical treatment of Esipov and Levinson [28] but with the addition of dynamic screening and allowance made for quasi-2D status. In using a temperature to describe the distribution function we implicitly assume that ee scattering is strong enough to establish an electron temperature but we do not assume that the distribution is drifted. The scattering rate for the process $\boldsymbol{k}_1 \rightarrow \boldsymbol{k}_1'$ in an isotropic Maxwellian distribution is:

$$W(\boldsymbol{k}_1, \boldsymbol{k}_1') = \frac{e^4 n}{8\pi\hbar A N_d} \int \exp\left(\frac{-E_2}{k_B T_e}\right) \frac{F^2(q)}{\varepsilon(\boldsymbol{q}, \omega)^2 q^2} \delta(E_1' + E_2' - E_1 - E_2) 2\,\mathrm{d}\boldsymbol{k}_2 \tag{1}$$

where n is the areal density of electrons, N_d is the effective density of states in the lowest subband, A is the area, $\hbar\boldsymbol{q}$ is the momentum transfer and $\varepsilon(\boldsymbol{q}, \omega)$ is the permittivity. The factor of two quantifies the exchange mechanism. Normal processes are assumed and the usual conservation of crystal momentum obviates the integration over $\boldsymbol{k}_2'$. Equation (1) is essentially that of Esipov and Levinson [28] with the quasi-2D form-factor and dynamic screening added. $F(q)$ is the form-factor, which for a heterostructure is:

$$F(q) = \int_0^\infty \mathrm{d}z \int_0^\infty \mathrm{d}z'\, \psi^2(z)\psi^2(z')\, \mathrm{e}^{-q|z-z'|} \tag{2}$$

where, in the case of a heterostructure, the z-dependent wavefunctions can be taken, for example, to be of Fang–Howard form [30]. Integration over $\boldsymbol{k}_2$ is straightforward. The integral over the angle between $\boldsymbol{k}_1$ and $\boldsymbol{k}_1'$ can be expressed in terms of a new variable:

$$u = \frac{q}{(k_1^2 - k_1'^2)^{1/2}} \tag{3}$$

so, after some manipulation and including the case for $k_1 < k_1'$ (corresponding to energy gain), we get:

$$\begin{aligned} W(k_1, k_1') &= W_0 \int_\gamma^{\gamma^{-1}} \frac{F^2(u)}{|\varpi|^{3/2}\{\varepsilon(u, \varpi)/\varepsilon_\infty\}^2} \mathrm{e}^{\varpi/2} \frac{\exp\left\{-\frac{|\varpi|}{4}\left(u^2 + \frac{1}{u^2}\right)\right\}}{u^2\left\{(u^2 - \gamma^2)\left(\frac{1}{\gamma^2} - u^2\right)\right\}^{1/2}} \mathrm{d}u, \\ W_0 &= \frac{e^4 n\hbar}{8\pi^{1/2}\varepsilon_\infty^2 m^*(k_B T_e)^2 A}, \gamma = \left|\frac{k_1 - k_1'}{k_1 + k_1'}\right|^{1/2} \end{aligned} \tag{4}$$

where ε_∞ is the high-frequency permittivity of the lattice and $\varpi = (E_1 - E_1')/k_B T_e$ is the normalized exchange energy. The energy-relaxation rate for the incident electron is then of the form:

$$Q = \int (E_1 - E_1') W(k_1, k_1') k_1'\, \mathrm{d}k_1' A/2\pi. \tag{5}$$

3. Screening

Dynamic effects enter into screening via the factor $\boldsymbol{q} \cdot \boldsymbol{v}_{cm}$, where $\boldsymbol{v}_{cm}$ is the velocity of the centre of mass [29]. It is straightforward to show that this factor is nothing but $(E_1 - E_1')/\hbar$ which is the frequency associated with the energy loss by the incident electron [26].

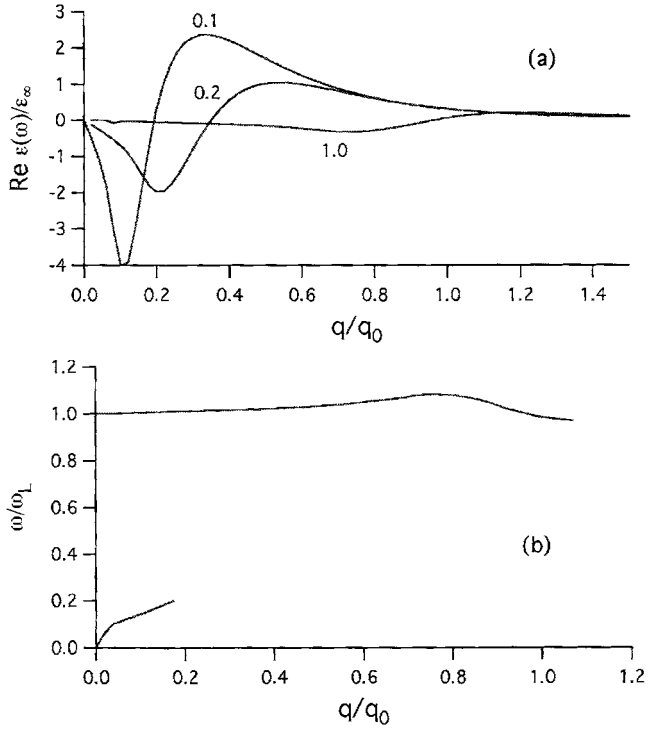

Figure 1. Plasma and coupled-mode effects (77 K, $n = 5 \times 10^{11}$ cm^{-2}). (a) The real part of the electron permittivity for $\omega/\omega_L = 0.1$, 0.2 and 1.0. (b) Plasmon and LO frequencies versus wavevector ($q_0 = (2m^*\omega_L)^{0.5}/\hbar$).

The permittivity is composed of the sum of lattice and electronic contributions. In a polar semiconductor the lattice contribution in the long-wavelength limit is:

$$\varepsilon_L(0,\omega) = \varepsilon_\infty \frac{\omega^2 - \omega_{LO}^2 + \mathrm{i}\omega\Gamma}{\omega^2 - \omega_{TO}^2 + \mathrm{i}\omega\Gamma} \tag{6}$$

where Γ is the decay rate. The electronic contribution can be obtained in the random-phase approximation neglecting the effects of exchange and correlation. A closed expression for the non-degenerate state has recently been obtained by Lee and Galbraith [25]. The real part is:

$$\varepsilon_{eR} = \frac{e^2 m^* n F(q)}{2\pi\hbar^2 N_d q^2}\left[A_+\Phi\left(1,\frac{3}{2},-\frac{\hbar^2 A_+^2}{2m^*k_BT_e}\right) + A_-\Phi\left(1,\frac{3}{2},-\frac{\hbar^2 A_-^2}{2m^*k_BT_e}\right)\right]$$
$$A_\pm = \frac{1}{2q}\left(q^2 \pm \frac{2m^*}{\hbar^2}\hbar\omega\right) \tag{7}$$

where $N_d = m^*k_BT_e/\pi\hbar^2$ is the 2D density of states and $\Phi(1, 3/2, -z)$ is a confluent hypergeometric function, and the imaginary part is:

$$\varepsilon_{eI} = \frac{e^2 m^* n F(q)}{2\pi\hbar^2 N_d q^2}\sqrt{\frac{\pi m^* k_B T_e}{2\hbar^2}}\left[\exp\left(-\frac{\hbar^2 A_-^2}{2m^*k_BT}\right) - \exp\left(-\frac{\hbar^2 A_+^2}{2m^*k_BT_e}\right)\right]. \tag{8}$$

The quantity that appears in the expression for the rate is the square modulus:

$$\varepsilon(q,\omega)^2 = (\varepsilon_{LR} + \varepsilon_{eR})^2 + (\varepsilon_{LI} + \varepsilon_{eI})^2. \tag{9}$$

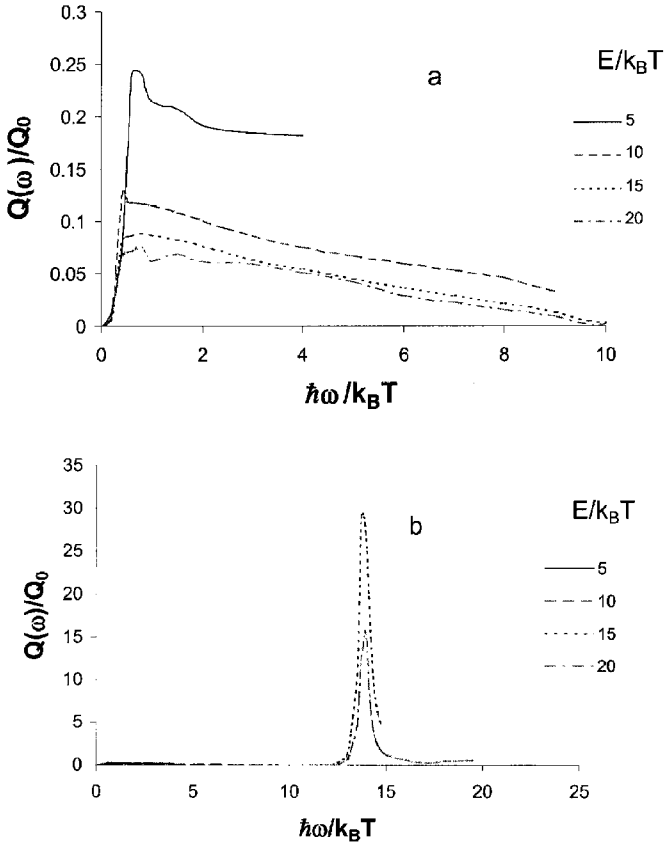

Figure 2. Energy-exchange rates for 2D GaN at 77 K for $n = 1 \times 10^{11}$ cm^{-2}: (a) low range, (b) high range ($Q_0 = 0.195$ eV ps^{-1}).

Let us consider the screening of quasi-elastic collisions with modest momentum transfer. Taking the argument of the confluent hypergeometric function to be small, we can expand and obtain:

$$\varepsilon_{eR} = \varepsilon_S \frac{q_s}{q}, \qquad \text{where } q_s = \frac{e^2 n F(q)}{2\varepsilon_s k_B T}. \tag{10}$$

Here, q_s is the 2D static screening vector. At the other extreme, we can consider the case of substantial energy exchange and take the asymptotic limit of the confluent hypergeometric function: $\phi(1, \frac{3}{2}, -z) \stackrel{z\to\infty}{\longrightarrow} \frac{1}{2z}$. The real part of the electron permittivity then can be expressed as follows:

$$\varepsilon_{eR} = \varepsilon_\infty \frac{\omega_{p\infty}^2}{\omega_q^2 - \omega^2}, \qquad \text{where } \omega_{p\infty}^2 = \frac{e^2 n F(q) q}{2\varepsilon_\infty m^*} \text{ and } \omega_q^2 = \frac{\hbar^2 q^4}{4m^{*2}}. \tag{11}$$

Here, $\omega_{p\infty}$ is the plasma frequency multiplied by the ratio of the static to the high-frequency permittivity and ω_q is assumed to be not too large. Resonances in the electron–electron interaction occur for energy exchanges that cause the real part of the permittivity to vanish. The corresponding frequencies are the roots of:

$$\omega^4 - \omega^2(\omega_L^2 + \omega_{p\infty}^2 + \omega_q^2) + \omega_L^2 \omega_q^2 + \omega_T^2 \omega_{p\infty}^2 = 0. \tag{12}$$

For modest electron densities, $\omega_{p\infty}^2 + \omega_q^2 \ll \omega_L^2$ and the solutions are:

$$\omega_+^2 = \omega_L^2 + \omega_{p\infty}^2 - \omega_{ps}^2 \qquad \text{and} \qquad \omega_-^2 = \omega_{ps}^2 + \omega_q^2 \tag{13}$$

where ω_{ps} is the plasma frequency $(e^2 n F(q) q/(2m^* \varepsilon_s))^{1/2}$. The higher-frequency resonance has been shifted upwards from the LO frequency by the difference involving the high-and low-frequency plasma terms. The lower-frequency resonance corresponds to the plasma frequency modified by dispersion. In both cases the real part of the screening function vanishes but the screening function itself remains finite because of the imaginary part. Thus, in the case of a non-degenerate electron gas, we expect to see an enhancement of the electron–electron interaction near the plasma frequency and near the LO phonon frequency.

A full numerical solution for the resonant frequencies shows that the approximations employed to reach equation (13) grossly underestimate the wavevector dependence. Figure 1 shows an example of this dependence for the real part of the electron permittivity and for the resonant frequencies (details to be found in section 5). In addition to the enhancements of the rate arising from dynamic screening there is also the wavevector and energy-exchange dependence of the integrand of equation (4) which favours the region around $u = 1$, so minimizing the argument of the exponential. The net spectrum can be expected to be richer than our approximate solution would suggest.

4. Energy exchange rates

The net energy exchange rate is determined mainly by substantial energy exchanges, even though these are not the most rapid. This may be seen by expressing equation (4) as follows (dropping the subscript 1):

$$W(k, k') = W_0 J_\pm(\varpi) \mathrm{e}^{\varpi/2} \tag{14}$$

where $J_\pm(\varpi)$ is the integral, which is dependent on the sign of the energy exchange through the denominator of γ (equation (4)). Noting that $\varpi > 0$ implies loss of energy and $\varpi < 0$ gain, we see that the net loss of energy by the incident electron is:

$$Q = Q_0 \left(\int_0^{E/k_B T} \varpi \mathrm{e}^{\varpi/2} J_+(\varpi)\, \mathrm{d}\varpi - \int_0^{\infty} \varpi \mathrm{e}^{-\varpi/2} J_-(\varpi)\, \mathrm{d}\varpi \right),$$

$$Q_0 = \frac{e^4 n}{16\pi^{3/2} \hbar \varepsilon_\infty^2} \tag{15}$$

where, now, ϖ is the magnitude of the energy exchanged and the subscript on E has been dropped.

Small energy exchanges contribute little to the integral (the factor $\varpi^{3/2}$ in the denominator of $J(\varpi)$ notwithstanding). When $\varpi \ll 1$, $J_+ \approx J_-$ and when $\varpi \gg 1$ the second integral in equation (15) is small and there will be little error in replacing the upper limit by $E/k_B T$. Thus, equation (15) can be simplified for superthermal electrons as follows:

$$Q = Q_0 \int_0^{E/k_B T} 2\varpi \sinh(\varpi/2) J_+(\varpi)\, \mathrm{d}\varpi. \tag{16}$$

5. Application to a GaN heterostructure

We illustrate the theory by choosing parameters for a GaN heterostructure, i.e. $m^* = 0.23$ m, $\varepsilon_\infty = 5.35\varepsilon_0$, $\varepsilon_s = 9.0\varepsilon_0$, $\hbar\omega_L = 92$ meV, $\hbar\omega_T = 71$ meV, $\Gamma = 1$ meV.

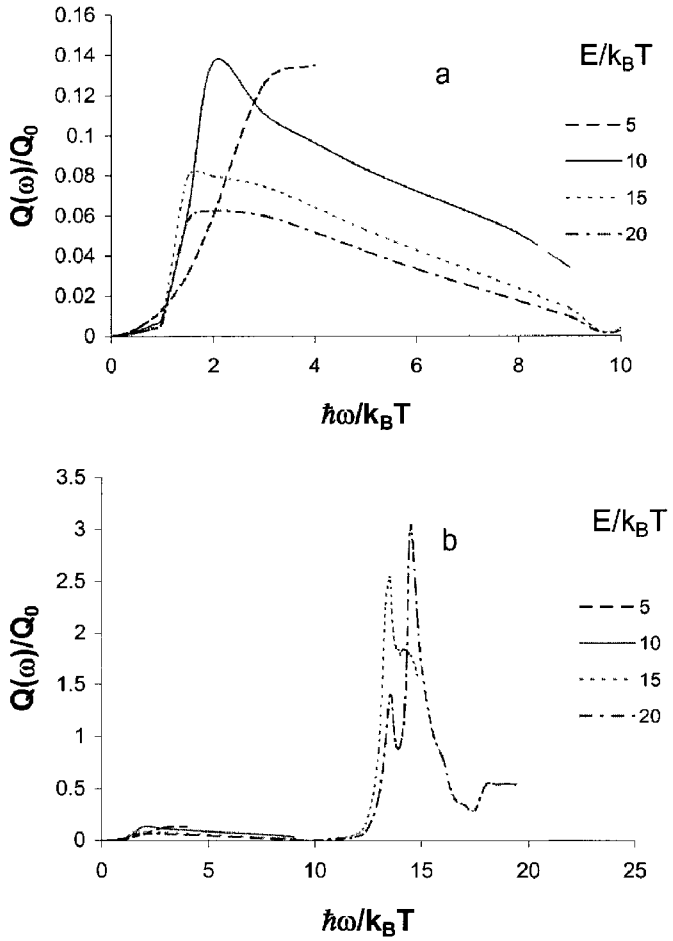

Figure 3. Energy-exchange rates for 2D GaN at 77 K for $n = 5 \times 10^{11}$ cm^{-2}: (a) low range, (b) high range ($Q_0 = 0.975$ eV ps^{-1}).

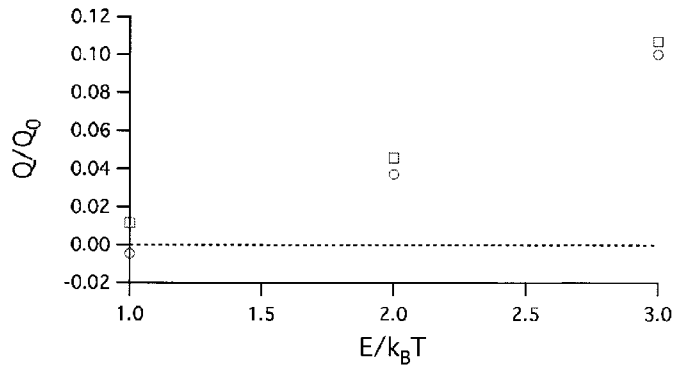

Figure 4. Net energy loss rates for near thermal electrons (GaN, 77 K, $n = 5 \times 10^{11}$ cm^{-2}): circles, without approximation; squares, with approximation.

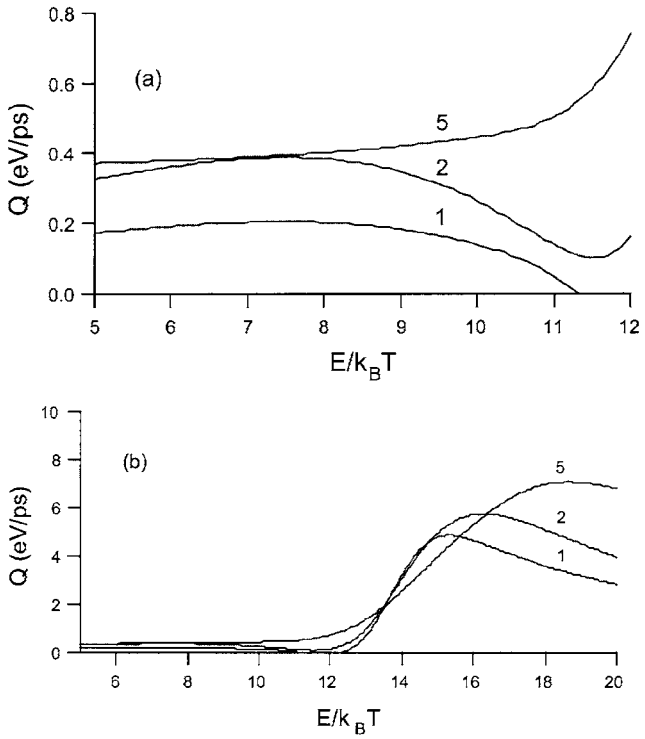

Figure 5. Energy-loss rates at 77 K in 2D GaN for superthermal electrons with energy E. The numbers on the curves refer to electron density in units of 10^{11} cm^{-2}: (a) low range, (b) high range.

Approximate analytical results for the strictly 2D case have been obtained with the assumption that the screening function and the integral in equation (4) can be evaluated for $u \approx 1$, which minimizes the argument of the exponential factor [26]. These results broadly bear out the expectations mentioned above. However, in what follows, we make no such approximations. The integral is evaluated numerically.

We consider first the strictly 2D case ($F(q) = 1$) and an electron temperature of 77 K. The spectrum of energy loss for an electron density of 1×10^{11} cm^{-2} is shown in figure 2 for several values of the energy of the incident electron. Superthermal values of incident energy are chosen to quantify the energy-exchange rate. This is a necessary choice since the net energy exchange for a thermal electron ($E/k_BT \approx 1$) is close to zero. The rates given in figure 2 are therefore the rates at which out-of-equilibrium electrons relax back into the thermal distribution and are the ones to compare with relaxation rates associated with other scattering mechanisms. Furthermore, the rates for large energy losses are essentially also the momentum-exchange rates.

The rates show two resonances as expected—a weak resonance at low exchange energies associated with the plasma frequency ($\hbar\omega_{ps}/k_BT \approx 0.8$) and a very strong resonance at an exchange energy very near to the LO phonon energy ($\hbar\omega_L/k_BT = 13.9$). Increasing the electron density to 5×10^{11} cm^{-2} shifts the low-energy maximum upwards ($\hbar\omega_{ps}/k_BT \approx 1.8$) and splits the high-energy resonance into two peaks (figure 3). The origin of the splitting is the dependence of the real part of the electron permittivity on wavevector relative to $q_0 = (2m^*\omega_L/\hbar^2)^{1/2}$. Roughly speaking, when $q > q_0$, ε_{eR} is positive and the real part

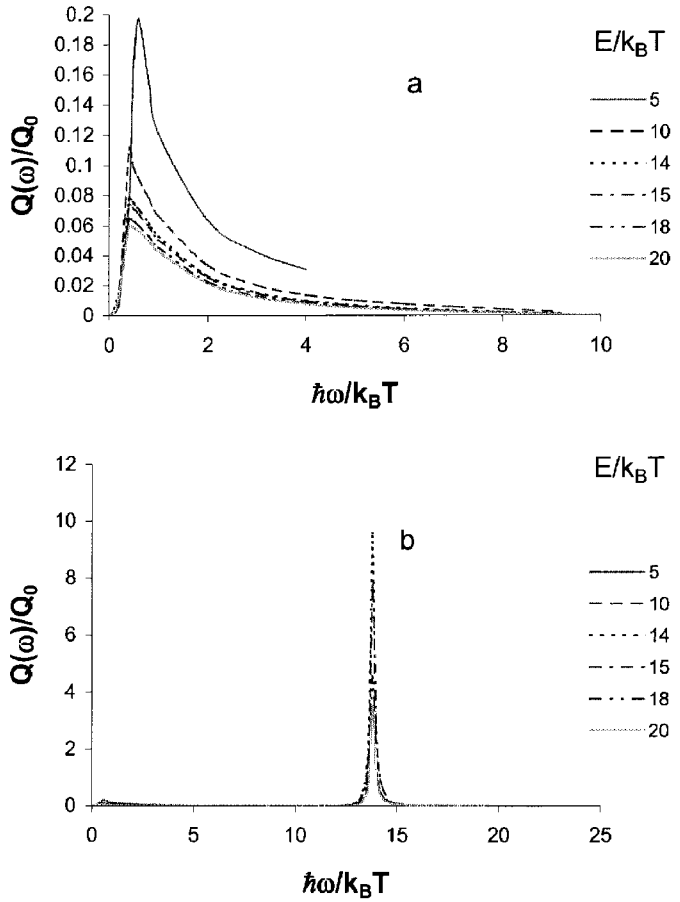

Figure 6. Energy exchange rates including form-factor for $n = 1 \times 10^{11}$ cm^{-2}: (a) low range, (b) high range.

of the total permittivity vanishes at a frequency somewhat below ω_L, whereas when $q < q_0$, $\varepsilon_{\varepsilon R}$ is negative so cancellation happens at a frequency somewhat above ω_L. The Maxwell–Boltzmann factor in the integrand of equation (4) maximizes at $u = 1$, which is equivalent to $q = q_0$, so both resonant frequencies appear with roughly comparable strengths. As one would expect, the splitting increases with electron density.

The net energy-exchange rate is given by equation (15). Performing the integrals numerically for the case $n = 5 \times 10^{11}$ cm^{-2} for near thermal incident electrons, we obtain the results shown by circles in figure 4 where they are compared with the results obtained from the approximate expression for superthermal electrons (equation (16)). The net rate should be zero for $E/k_BT = 1$: the small negative result shown by the circle indicates the level of numerical error. Apart from the case $E/k_BT = 1$, the approximate expression gives results of sufficient accuracy.

Integrating over the energy-exchange spectral function (equation (16)) gives the net rate of loss of energy for superthermal electrons. Figure 5 shows the results for electron densities 1, 2 and 5×10^{11} cm^{-2} (the latter density at the limit for non-degeneracy). A large increase occurs for electrons with initial energies near and greater than the phonon energy ($\hbar\omega_L/k_BT = 13.9$).

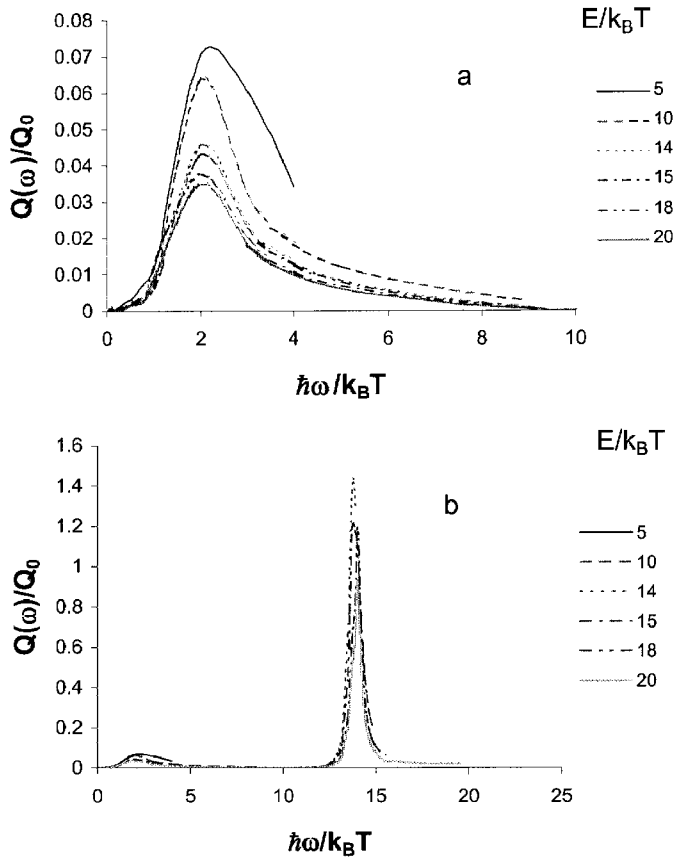

Figure 7. Energy exchange rates including form-factor for $n = 5 \times 10^{11}$ cm^{-2}: (a) low range, (b) high range.

It is notable that the highest rates are comparable with the 2D emission rate associated with the optical phonons in GaN ($\approx$9 eV ps^{-1}). The rates for energy exchanges less than the phonon energy are much smaller. A time constant can be associated with the energy loss rate via

$$\frac{1}{\tau} = W_E = \frac{Q}{E}. \tag{17}$$

As previously mentioned, this rate can be taken to be the momentum relaxation rate for purposes of comparison with other rates.

All of the above results are for the strictly 2D case. Including the quasi-2D nature affects the rates by the q-dependent form-factor which, of course, depends on the details of the quantum well. Figures 6 and 7 illustrate the effect of including the form-factor for the case of a triangular well and a Fang–Howard wavefunction [30]: $\psi(z) = (b^3/2)^{1/2} z \mathrm{e}^{-bz/2}$ with $b = 4.8 \times 10^6$ m^{-1}:

$$F(q) = \frac{8 + 9(q/b) + 3(q/b)^2}{8[1 + (q/b)]^3}. \tag{18}$$

Near the phonon resonance the wavevector is $q_0 = (2m^*\omega_L/\hbar^2)^{1/2}$, which would lead to $F(q) \approx 0.2$. Thus, a reduction by a factor of five might be expected but it turns out that rates are reduced by a factor of only three or four (roughly). The reason for this smaller

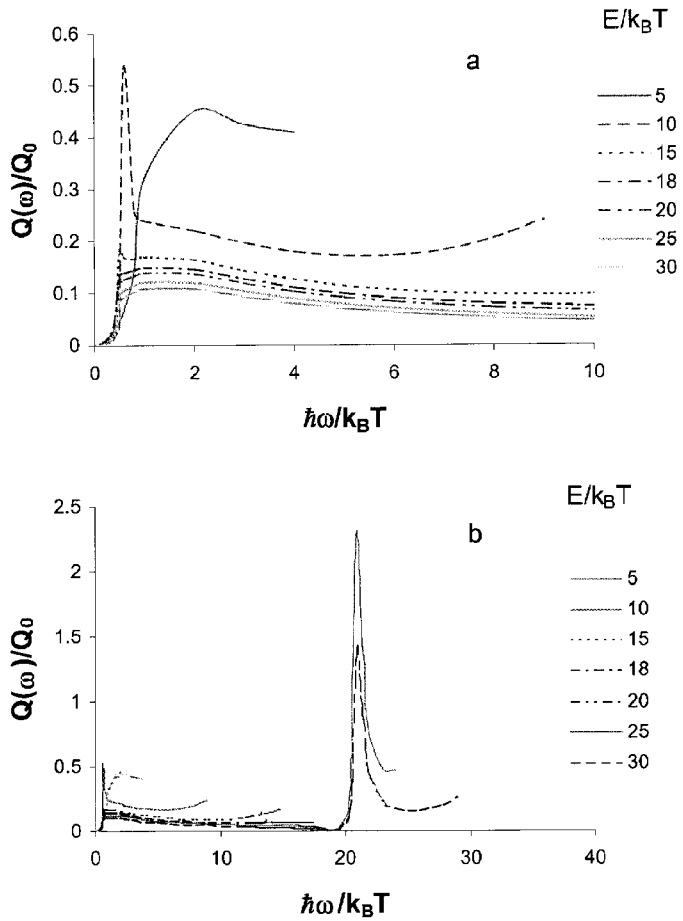

Figure 8. Energy exchange rates in 2D GaAs for $n = 2 \times 10^{10}$ cm^{-2}: (a) low range, (b) high range.

reduction is that substantial contributions to the rate are associated with the resonances where the real part of the dielectric function vanishes, leaving the screening to be determined by the imaginary part. This is dominated by the electronic component which means that the squared form-factor tends to cancel out. Similar considerations explain the insensitivity of the energy exchange rates to electron density once the density is high enough. The effect of including the form-factor for the low-energy range is significantly smaller because smaller values of q are involved.

In our example the 2D low-energy rate for the upper value of density is about 1×10^{13} s^{-1}, so in cases where the mobility is much greater than $e/(W_E m^*) \approx 800$ cm^2 V^{-1} s^{-1} we can expect the hot-electron distribution to be a drifted Maxwellian. Including the form-factor reduces the rate by roughly a factor of two and increases the mobility to 1600 cm^2 V^{-1} s^{-1}. It is interesting to notice that the introduction of the form-factor to the bare optical-phonon interaction reduces the strength by a factor of five (roughly), making the energy relaxation rates for optical-phonon scattering and ee scattering comparable.

We have looked briefly at the situation in 2D GaAs choosing an appropriately lower temperature (20 K). Figure 8 shows the energy-loss spectrum for an electron density of

2×10^{10} cm^{-2}. Under these conditions the phonon resonance is quite sharp. In general, the spectrum is similar to that for GaN.

The establishment of a drifted Maxwellian will, of course, affect the electron–electron energy and momentum rates. We make no attempt to address this effect here.

6. Summary

We have examined in some detail the effect that dynamic screening has on the rate of energy exchange in electron–electron collisions. The rate is significantly increased when the exchange energy is near to either the plasmon or the optical-phonon energies. Rates are calculated for non-degenerate electrons in GaN at 77 K and for GaAs at 20 K. It is shown that the energy-exchange rates can be comparable to the energy-relaxation rate associated with the emission of optical phonons.

Acknowledgment

We are grateful for the financial support of the Office of Naval Research via grant N00014-01-1-0002 sponsored by Dr Colin Wood.

References

[1] Dahl D A and Sham L J 1977 *Phys. Rev.* B **16** 651
[2] Maldague P F 1978 *Surf. Sci.* **73** 296
[3] Ando T, Fowler A B and Stern F 1982 *Rev. Mod. Phys.* **54** 437
[4] Lee J and Spector H N 1983 *J. Appl. Phys.* **54** 6989
[5] Bechstedt F and Enderlein R 1985 *Phys. Status Solidi* b **131** 53
[6] Lei X L 1985 *J. Phys. C: Solid State Phys.* **18** L593
[7] Esipov S E 1986 *Sov. Phys.–JETP* **63** 1319
Esipov S E 1987 *Sov. Phys.–JETP* **65** 610
[8] Das Sarma S 1986 *Phys. Rev.* B **33** 5401
[9] Bailey D W, Artaki M A, Stanton C J and Hess K 1987 *J. Appl. Phys.* **62** 4368
[10] Goodnick S M and Lugli P 1988 *Solid State Electron.* **31** 463
[11] Blom P W M, Smit C, Haverkort J E M and Wolter J H 1993 *Phys. Rev.* B **47** 2072
[12] Mosko M, Moskova A and Cambel V 1995 *Phys. Rev.* B **51** 16860
[13] Lyn J J and Bird J P 2002 *J. Phys.: Condens. Matter* **14** R501
[14] Fröhlich H and Paranjape B V 1956 *Proc. Phys. Soc.* B **69** 21
[15] Stratton R 1957 *Proc. R. Soc.* A **242** 355
Stratton R 1958 *Proc. R. Soc.* A **246** 406
[16] See for example
Ridley B K 1991 *Rep. Prog. Phys.* **54** 169
[17] Bernardini F, Fiorentini V and Vanderbilt D 1997 *Phys. Rev.* B **56** R10024
[18] Ambacher O, Smart J, Shealy J R, Weimann N G, Chu K, Murphy M, Schaff W J, Eastman L F, Dimitrov R, Wittmer L, Stutzmann M, Rieger W and Hilsenbeck J 1999 *J. Appl. Phys.* **85** 3222
[19] Ridley B K 2000 *Appl. Phys. Lett.* **77** 990
[20] Ridley B K and Zakhleniuk N A 2000 *Int. J. High Speed Electron. Syst.* **11** 479
Brennan K F and Ruden P P (ed) 2001 *Topics in High Field Transport in Semiconductors* (Singapore: World Scientific) p 117
[21] See for example
Reggiani L 1985 *Hot-Electron Transport in Semiconductors* (Berlin: Springer)
Shah J (ed) 1992 *Hot Carriers in Semiconductor Nanostructures* (New York: Academic)
[22] Tripathi P and Ridley B K 2002 *Phys. Rev.* B **66** 1553XX
[23] Collet J H 1993 *Phys. Rev.* B **47** 10279

[24] Kane M G 1996 *Phys. Rev.* B **54** 16345
[25] Lee S-C and Galbraith I 1999 *Phys. Rev.* B **59** 15796
Lee S-C and Galbraith I 2000 *Phys. Rev.* B **62** 15327
[26] Ridley B K 2001 *J. Phys.: Condens. Matter* **13** 2799
[27] Tavares M R S, Hai G-Q and Das Sarma S 2001 *Phys. Rev.* B **64** 045325
[28] Esipov S E and Levinson I B 1986 *Sov. Phys.–JETP* **63** 191
[29] Meyer J R and Bartoli F J 1983 *Phys. Rev.* B **28** 915
[30] Fang F F and Howard W E 1996 *Phys. Rev. Lett.* **16** 797